Coherence effects in the scattering from domain structures

2007 J. Phys.: Condens. Matter 19 275206

(http://iopscience.iop.org/0953-8984/19/27/275206)

IOP PUBLISHING JOURNAL OF PHYSICS: CONDENSED MATTER

J. Phys.: Condens. Matter **19** (2007) 275206 (11pp) doi:10.1088/0953-8984/19/27/275206

Coherence effects in the scattering from domain structures

H Boysen

Department of Geo- and Environmental Sciences, Section Crystallography, Theresienstraße 41, 80333 München, Germany

E-mail: Boysen@lmu.de

Received 19 December 2006, in final form 19 January 2007
Published 1 June 2007
Online at stacks.iop.org/JPhysCM/19/275206

Abstract

Scattering techniques with x-rays or neutrons are most effective for studying domain and domain wall structures on a mesoscopic scale. For small domain sizes and small strains between adjacent domains, coherence effects can give rise to significant modifications of the scattering intensity distribution which cannot generally be neglected. Additional or missing peaks, peak shifts and peak narrowing can lead to false conclusions concerning assignments to multiple phases, lower or higher symmetries, wrong lattice constants and domain sizes, respectively. This is demonstrated by examples calculated with a simple scattering theory outlined.

(Some figures in this article are in colour only in the electronic version)

1. Introduction

Domain structures arising from structural phase transitions play an important role in the characteristics of solids. In ferroelectric and ferroelastic materials they determine their physical properties; in minerals they contain information about the thermal history of rocks, etc. Salje (1990) gives a comprehensive overview of the formation and appearance of such microstructures consisting of (twin) domains and the walls between them. Experimentally they may be studied by optical, electron microscopical or other methods. The most complete and reliable information is, however, obtained from non-destructive diffraction methods using x-rays or neutrons. A recent review on the application of these latter methods was presented by Hayward and Salje (2005), where references to the original literature may also be found.

The corresponding diffraction theory has been worked out and discussed by several authors using either direct analytical solutions or applying numerical simulations. A general (but unspecific) formulation was outlined by Boysen (1995) using the concept of Fourier transforms and convolutions. There it was also pointed out that the general formulae for the scattering intensities contain interference terms due to coherence effects between adjacent domains and

domain walls. As will be seen below, for planar interfaces the diffraction problem can be regarded as a stacking of ordered planes, where the interface between adjacent domains forms a stacking fault. Hence, among others (see Jagodzinski and Frey 1996), the general diffraction theory for crystals with planar faults worked out by Cowley (1976) could be applied. Cowley and Au (1978) have already emphasized the importance of coherence effects in the study of microtwins on a mesoscopic scale of several hundreds of angstroms. A detailed diffraction theory for a pair of twin domains was developed by Bruce (1981) and extended by Andrews and Cowley (1986), who considered both an infinitely thin domain wall and an extended wall with constant lattice spacing. In real samples, however, one has to take into account a variation of the lattice spacing within the walls due to the relaxation of strains (Salje 1990). A widely accepted form of the variation of the strain within the wall was derived from continuum elastic theory by Barsch and Krumhansl (1984):

$$e(x) = e_0 \tanh(x/W), \tag{1}$$

where e_0 is the strain deep within the proper domains, $2W$ can be defined as the width of the wall and x is the coordinate perpendicular to the wall. This relation generally applies for small strains; for larger strains higher-order correction terms have been given by Jacobs (1985). Although the validity of the continuum approach may be (and has been) questioned for small wall widths of only a few lattice constants (usually less than 6; see the compilation of Hayward and Salje 2005), (1) will be used in the following for simplicity, since the main objectives of this work are the coherence aspects of the scattering, which are only little affected by the actual form of the strain variation. Indeed (1) has been applied by most authors for the analysis of experimental diffraction data. Apart from numerical simulation studies, simplified analyses were presented by Taylor and Swainson (1998) and Boysen (2005) for the case of powder diffraction. These authors have calculated the probability densities of the occurrences of the different unit cell orientations or lattice spacing, respectively, by differentiation of (1) and summed up the corresponding intensities. This approach ignores the coherence effects and may be justified in real systems, if one takes into account possible variations of domain sizes, wall widths, the existence of rough interfaces, dislocations, defects, etc, which all tend to smear out the coherence between individual pairs. In fact, these approximations have been quite successful in describing the asymmetry and anisotropic broadening of the peaks observed experimentally. As will be shown, however, another requirement is that the domain sizes and strains should not be too small, since otherwise coherence effects must not be neglected.

Surprisingly, in spite of the fact that the diffraction theory is well known, the inherent interference effects seem to have been overlooked or ignored in many interpretations of experimental data. This has recently been demonstrated again by Khoshnevisan *et al* (2002) in a study of the tetragonal to orthorhombic phase transition in YBCO by powder diffraction methods. By analytical and simulation studies they found that for specific values of the domain sizes (lateral extension) and strains, additional peaks between twin-related reflection pairs can show up, which may be misinterpreted as arising from the high-symmetry structure, which is in fact not present in the sample as a separate phase. The intention of this contribution is to rationalize these effects. To do this, the diffraction theory has been reformulated by separating the contributions from the domains, the wall and the interference term. This can be done analytically for infinitely thin domain walls, and this will be the main concern in the following. Additional effects due to finite wall extensions will briefly be discussed via numerical calculations. It will be shown that indeed additional or fewer peaks and shoulders as well as peak shifts and narrowing may arise under certain circumstances, which can lead to erroneous assignments to multiple phases, lower or higher symmetries and wrong lattice constants and domain sizes, respectively.

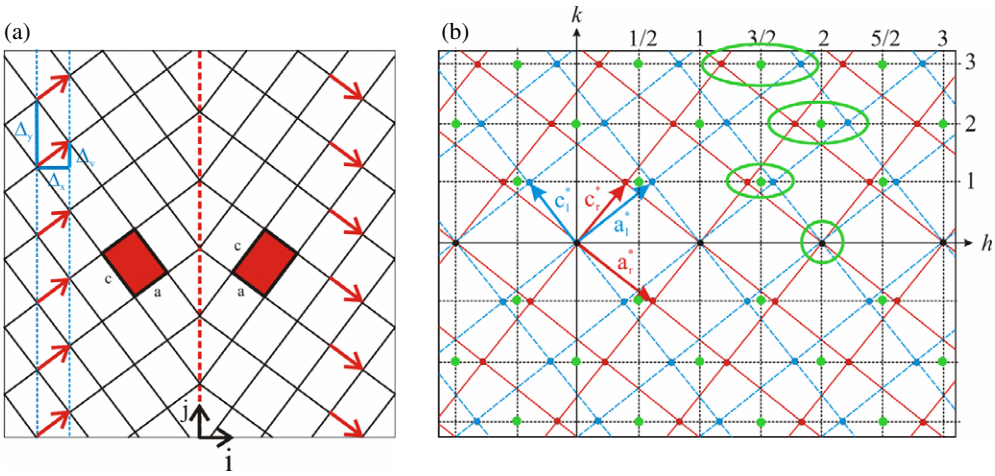

Figure 1. (a) Model of two twin-related domains separated by a single interface plane (dotted line). The arrows indicate the shifts of the well-ordered planes parallel to the wall. For illustration purposes the strain has been exaggerated unrealistically. (b) Reciprocal lattices corresponding to (a). High-symmetry reflection positions are marked by (green) circles on the square grid. The symbols are explained in the text.

2. Scattering theory

As mentioned, for simplicity the discussion will be restricted to the general characteristics of the interference terms. Therefore, the scattering theory will be outlined only for a simple monatomic structure, i.e. the variation of the structure factor along the scattered intensity as well as the influence of the instrumental resolution function (which will smear out the small side maxima seen in the figures below) will be neglected. Moreover, the model consists of only two domains separated by a single wall. If the domains are spaced very regularly, additional satellite peaks may appear. All this has to be kept in mind when trying to apply the derived formulae to any real situation.

First we consider the case of an infinitely thin domain wall. Figure 1(a) shows the model of two twin domains; figure 1(b) shows the corresponding reciprocal lattices. For illustrative purposes we refer to two tetragonal domains arising from a phase transition from a parent cubic structure with the domains separated by {101} walls. We define a coordinate system **i** perpendicular to the wall, **j** parallel to the wall and **k** perpendicular to the drawing plane. As can be seen, the model can be regarded as consisting of well-ordered planes extended along **j** and **k** (with translation periods Δ_y and Δ_z) stacked along **i** with constant spacing Δ_x but shifted along **j** by Δ_v, the latter being reversed at the twin boundary (indicated by the arrows in figure 1(a)). Then the lattice points are located at $\mathbf{r}_\mathrm{l} = n\Delta_x\mathbf{i} + n\Delta_v\mathbf{j} + n'\Delta_y\mathbf{j} + n''\Delta_z\mathbf{k}$ for the left domain, $\mathbf{r}_\mathrm{r} = n\Delta_x\mathbf{i} - n\Delta_v\mathbf{j} + n'\Delta_y\mathbf{j} + n''\Delta_z\mathbf{k}$ for the right domain and $\mathbf{r}_0 = \mathbf{0} + n'\Delta_y\mathbf{j} + n''\Delta_z\mathbf{k}$ for the single interface plane (the domain wall). In our tetragonal example the shifts are $\Delta_x = ac/\Delta_y$, $\Delta_v = a^2/\Delta_y$ and $\Delta_y = \sqrt{a^2 + c^2}$. Similar relations can easily be derived for other geometries, such that the Δ can also be taken as some general values in the following. Assuming large extensions of the planes parallel to the wall, the structure factor of these planes can be calculated separately by summations over n' and n'' leading to the corresponding lattice functions in k and l, i.e. the reflections are 'sharp' along **j** and **k**. The Miller indices h, k and l of the chosen coordinate system are defined with respect to the high-symmetry state (for which $\Delta_x = \Delta_v = \Delta_y/2$) with reciprocal lattice axes along **i**, **j** and **k** in units of $1/\Delta_x$, $1/\Delta_y$ and

$1/\Delta_z$, respectively (see figure 1(b)). Hence k and l can assume only integer values, while h is a continuous variable. In our illustrative example

$$h = (h_{\mathrm{l/r}}c^2 \mp l_{\mathrm{l/r}}a^2)/(a^2 + c^2) \qquad \text{and} \qquad k = (\pm h_{\mathrm{l/r}} + l_{\mathrm{l/r}}), \tag{2}$$

where $h_{\mathrm{l/r}}$ and $l_{\mathrm{l/r}}$ are the usual tetragonal indices and the upper and lower signs refer to the left and right domain, respectively.

Since the intensity varies only along h, we have to treat only a simple one-dimensional problem. The corresponding structure factor can be separated into three terms, the summations over both domains and the wall:

$$F(h) = \sum_{n=-N}^{-1} \exp[2\pi \mathrm{i}(n\Delta_x\xi + n\Delta_v\eta)] + \sum_{n=1}^{N} \exp[2\pi \mathrm{i}(n\Delta_x\xi - n\Delta_v\eta)] + 1, \tag{3}$$

where $\xi = h/\Delta_x$ and $\eta = k/\Delta_y$. N is the number of planes in each domain of equal size (length) $L = N\Delta_x$ and $2N + 1$ is the total number of planes. The first two terms can be evaluated in the usual way involving the (roots of) Laue functions of order N (times the phase factors governing the interference effects):

$$S_{\mathrm{l}} = \frac{\sin[\pi N(\Delta_x\xi + \Delta_v\eta)]}{\sin[\pi(\Delta_x\xi + \Delta_v\eta)]} \qquad \text{and} \qquad S_{\mathrm{r}} = \frac{\sin[\pi N(\Delta_x\xi - \Delta_v\eta)]}{\sin[\pi(\Delta_x\xi - \Delta_v\eta)]}. \tag{4}$$

The intensity is given by the absolute square FF^* and can be separated into four terms:

$$I = S_{\mathrm{l}}^2 + S_{\mathrm{r}}^2 + 1 + S_{\mathrm{int}}. \tag{5}$$

The first three terms are the squares of the three terms in (3), i.e. S_{l}^2 and S_{r}^2 are the intensities from both domains separately and '1' is the (constant) intensity from the interface (twin plane). The interference term arises from the remaining cross products and is given by

$$\begin{aligned} S_{\mathrm{int}} = 2\{&S_{\mathrm{l}}S_{\mathrm{r}}\cos[2\pi(N+1)\Delta_x\xi] + S_{\mathrm{l}}\cos[\pi(N+1)(\Delta_x\xi + \Delta_v\eta)] \\ &+ S_{\mathrm{r}}\cos[\pi(N+1)(\Delta_x\xi - \Delta_v\eta)]\} \end{aligned}$$

which can be simplified to

$$S_{\mathrm{int}} = 2\{S'_{\mathrm{l}}S'_{\mathrm{r}}\cos[2\pi N\Delta_x\xi] - 1\}, \tag{6}$$

where S'_{l} and S'_{r} are Laue functions of order $N + 1$. In terms of $h = \xi\Delta_x$ and $k = \eta\Delta_y$,

$$S_{\mathrm{int}}(h) = 2\left\{\frac{\sin[\pi(N+1)(h+rk)]}{\sin[\pi(h+rk)]}\frac{\sin[\pi(N+1)(h-rk)]}{\sin[\pi(h-rk)]}\cos(2\pi Nh) - 1\right\}, \tag{7}$$

where $r = \Delta_v/\Delta_y \approx (1 + e)/2$ is related to the strain defined as $e = (\Delta_v - \Delta_x)/\Delta_x$.

This function has maxima and minima leading to the addition/subtraction of intensity to/from the Laue terms S_{l}^2 and S_{r}^2 having their maxima at $h_{\mathrm{l/r}} = m \pm rk$, or, in terms of the strain, $h_{\mathrm{l/r}} = m \pm \frac{e}{2}k$ for k even and $h_{\mathrm{l/r}} = m + \frac{1}{2} \pm \frac{e}{2}k$ for k odd with $m =$ integer (cf figure 1(b)). Since S_{int} is periodic in h, it is sufficient to consider only small regions (some of them encircled in figure 1(b)) around the positions of the high-symmetry reflections $h_0 = m$ or $m + \frac{1}{2}$ for k even or odd, respectively. Then with $\Delta h = h - h_0$

$$S_{\mathrm{int}}(\Delta h) = 2\left\{\frac{\sin[\pi(N+1)(\Delta h + \frac{e}{2}k)]}{\sin[\pi(\Delta h + \frac{e}{2}k)]}\frac{\sin[\pi(N+1)(\Delta h - \frac{e}{2}k)]}{\sin[\pi(\Delta h - \frac{e}{2}k)]}\cos(2\pi N\Delta h) - 1\right\}, \tag{8}$$

which is symmetric around $\Delta h = 0$ and can be confined to $|\Delta h| \leqslant ek$. For very large N the *relative* contribution of S_{int} is small compared to S_{l}^2 and S_{r}^2 (of the order of $1/N$) and may be neglected in most practical situations, i.e. the usual incoherent superposition of intensities

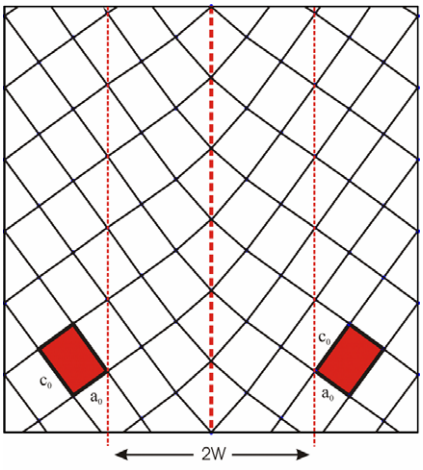

Figure 2. Same as figure 1(a), but with a finite extension of the domain wall (dotted lines).

is sufficient to describe experimental data in this case. This is no longer true if N becomes smaller. There is always a maximum at $\Delta h = 0$ with intensity

$$S_{\text{int}}(0) = 2\left\{\frac{\sin^2[\pi(N+1)\frac{e}{2}k]}{\sin^2[\pi\frac{e}{2}k]} - 1\right\}, \tag{9}$$

which may become very large and even exceed that of the proper twin reflections (whose intensities are $\propto N^2$) for small values of Nek (less than one to be specific), i.e. small domain extensions, small strains and not too large k. Moreover, further maxima of comparable intensities not coinciding with $h_{1/\text{r}}$ or h_0 may appear. For a typical strain of $e \approx 0.02$, $N \approx 1/ek$ may be as large as about 50, corresponding to a domain size of several hundreds of angstroms. Clearly, the coherence effects become less important with increasing k. All this will be demonstrated in the examples below.

The case of a finite extension of the domain wall with a strain variation according to (1) is illustrated in figure 2. There are still ordered planes along **j** and **k** and the stacking period Δ_x along **i** is constant, but the shifts along **j** are modified within the wall. The lattice points are now given by $\mathbf{r} = n\Delta_x\mathbf{i} + [\pm n\Delta_x + u(n)]\mathbf{j} + n'\Delta_y\mathbf{j} + n''\Delta_z\mathbf{k}$, where the upper and lower signs correspond to the left and right domain, respectively. The displacements relative to the high-symmetry lattice are obtained by integration of (1):

$$u(n) = e_0 W \ln\cosh(x/W) = e_0 n_w \Delta_x \ln\cosh(n/n_w), \tag{10}$$

where the width of the wall $W = n_w\Delta_x$ is counted in units of Δ_x. As before, the reflections are 'sharp' along **j** and **k**, and the structure factor along **i**

$$F(h) = \sum_{n=-N}^{N} \exp\left\{2\pi\text{i}\left[nh + \frac{\Delta_x}{\Delta_y}(\pm n + e_0 n_w \ln\cosh(n/n_w))k\right]\right\} \tag{11}$$

could be separated into contributions from the domains, the domain wall and the interference term, but no simple solution as in the previous case was found. Therefore, only some numerical calculations using (11) will be shown to demonstrate the minor influence of an extended domain wall on the coherence effects.

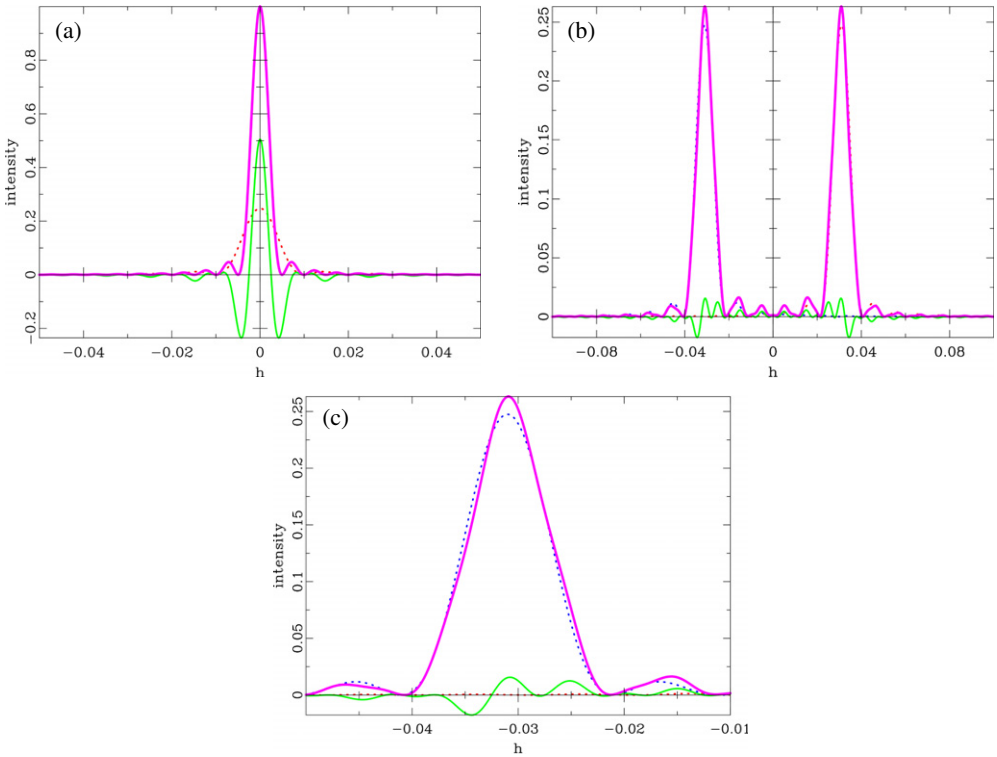

Figure 3. Calculated intensities of separate domains S_l^2 and S_r^2 (dashed lines, red and blue), interference term S_{int} (solid line, green) and total intensity I (thick solid line, purple) for $e = 0.064$, $N = 100$ and (a) $k = 0$, (b) $k = 1$. (c) is an enlarged section of (b).

3. Examples and discussion

In the following some examples are given to illustrate the features that follow from the results derived above. To be specific, two examples of strains will be considered which apply to the (improper) ferroelastic (ferroelectric) phase transition $Pm3m \rightarrow P4mm$ in $PbTiO_3$ (Boysen 2005). At room temperature $a = 3.902$ Å, $c = 4.152$ Å ($e = 0.064$) and at 740 K $a = 3.958$ Å, $c = 4.007$ Å ($e = 0.012$). From the condition following (9), Nek less than ≈1, coherence effects should be strong for $N \approx 15$ at room temperature and for $N \approx 80$ at 740 K. For N much larger than these they should be negligible. This is illustrated in figure 3 for $e = 0.064$ and $N = 100$. Here and in the following figures the dashed lines represent the individual intensities from both domains S_l^2 and S_r^2, the thin solid line the interference term S_{int} and the thick solid line the total intensity I. All intensities are normalized with respect to the total number of planes by division through $(2N + 1)^2$. Figure 3(a) shows the result for $k = 0$ which implies $h =$ integer. Here, of course, S_{int} is very strong (cf (7)) and correctly leads to a final Laue function of order $2N + 1$, as $k = 0$ corresponds to a projection along **j**, which is of course well ordered. As expected, for $k = 1$ (figure 3(b)) I and the sum of S_l^2 and S_r^2 are almost identical, although there are slight differences as seen in the magnified picture (figure 3(c)), too small, however, to be observed experimentally. Figure 4 shows the case when N is reduced to 15. For $k = 1$ (figure 4(a)) there is an additional strong central peak, which is mainly due to S_{int} and not simply due to the superposition of S_l^2 and S_r^2. Furthermore, the first side

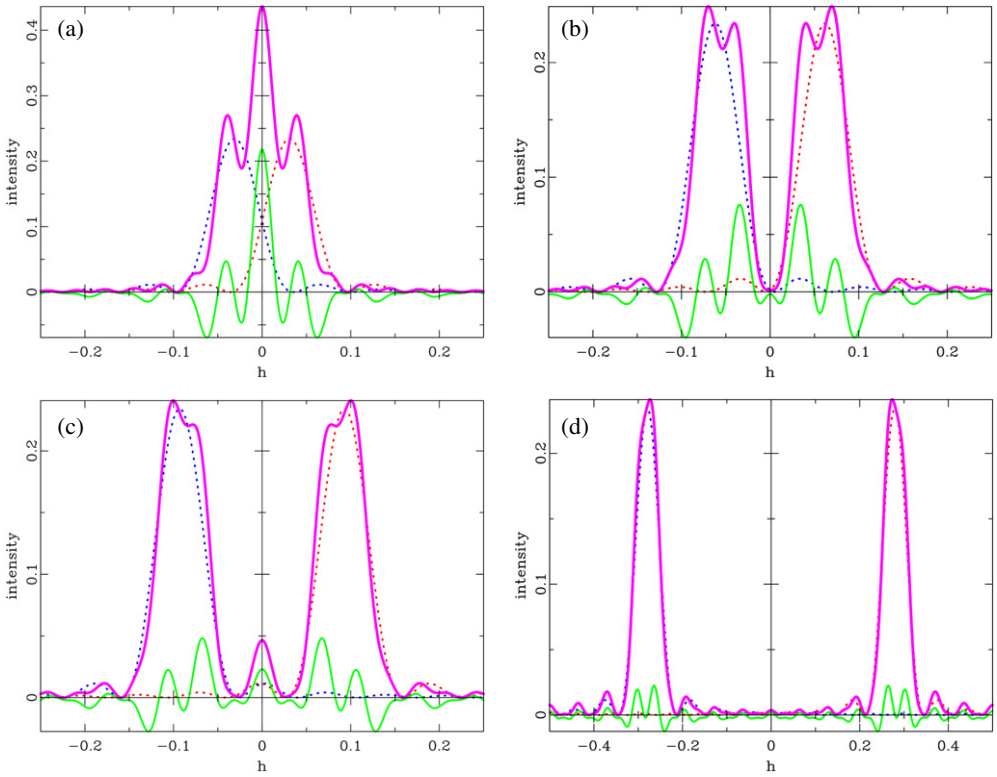

Figure 4. Same as figure 3 for $e = 0.064$, $N = 15$ and (a) $k = 1$, (b) $k = 2$, (c) $k = 3$, (d) $k = 9$.

peaks of S_{int} have enough intensity to shift the positions of the proper domain peaks, and the minima lead to an apparent sharpening of all peaks. As a consequence, from the appearance of the total intensity pattern alone one may be led to the false conclusion that there are two phases (tetragonal and cubic in our case), derive wrong lattice constants from the shifted peak positions and a too large extension of the domains from the narrowed peak widths. For $k = 2$ (figure 4(b)) there is no central peak, but the proper domain peaks appear to be split, which again may lead to the assumption of two phases or lower symmetry. For $k = 3$ (figure 4(c)) the central peak reappears and the domain peaks remain split, i.e. a complicated five-peak structure results, completely further obscuring the true situation. Only for very large values of k is the 'normal' two peak structure recovered (figure 4(d)).

While the previous case is certainly unrealistic with a very large strain and a very small domain size of N only 15, very similar features result for other combinations of N and e with roughly equal products Ne. So the smaller strain $e = 0.012$ allows larger and more realistic values of N. Figure 5 shows the dependence on (large) variations of N for $k = 2$. For $N = 1000$ there is a two-peak structure practically identical with the incoherent case, for $N = 100$ a three-peak structure with the twin peaks roughly at the correct positions (leading to the false conclusion of the coexistence of low- and high-symmetry phases) and for $N = 15$ only one peak at the central position (leading to the false conclusion that the material is in the high-symmetry phase). Note again that in the latter case the peak is much sharper than the simple superposition of S_{l}^2 and S_{r}^2 wrongly suggesting even larger domains of the high-symmetry phase. Figure 6(a) shows the situation for a small variation of N around $N = 50$. As

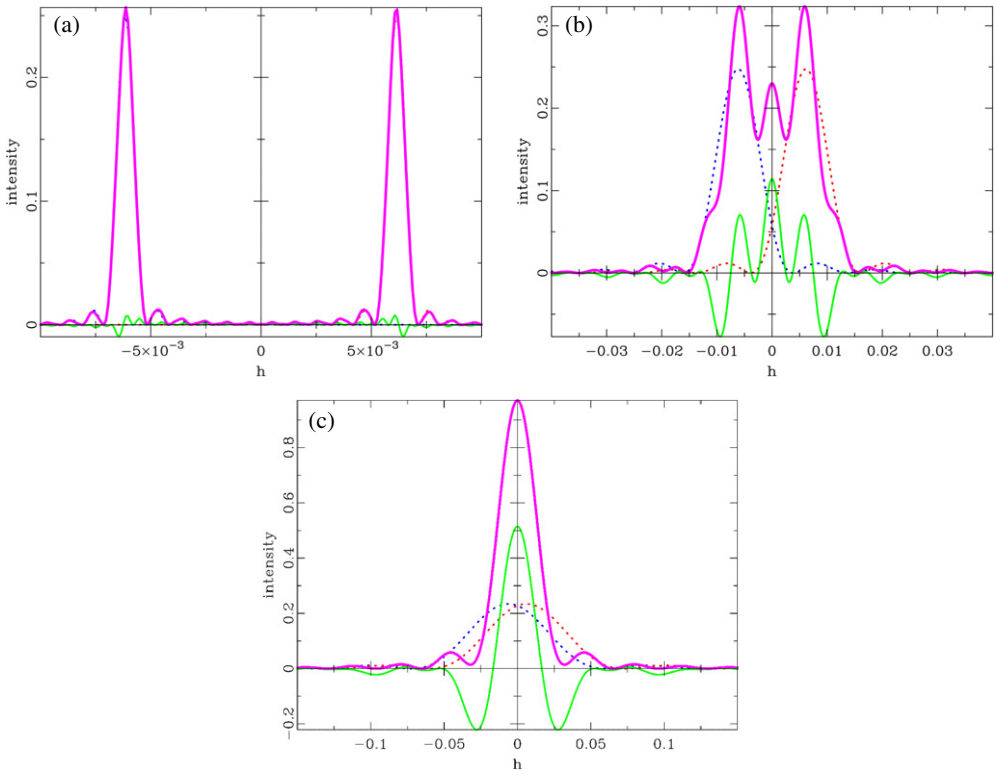

Figure 5. Same as figure 3 for $e = 0.012$, $k = 1$ and (a) $N = 1000$, (b) $N = 100$, (c) $N = 15$.

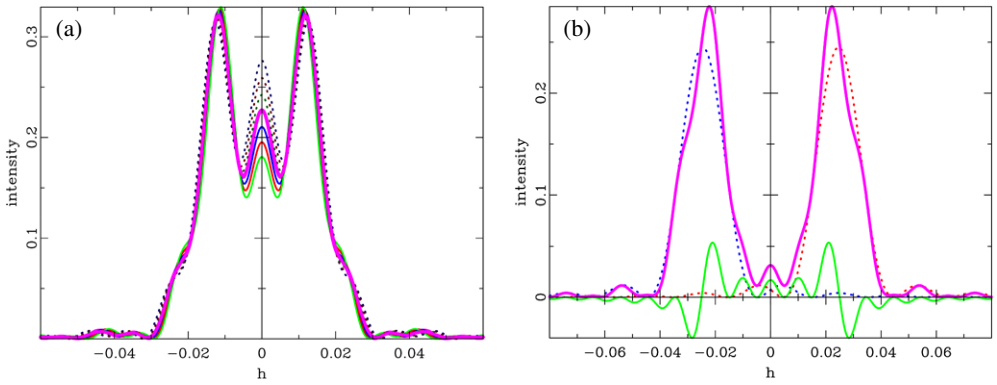

Figure 6. Same as figure 3 for $e = 0.012$, $N = 50$ and (a) $k = 2$, (b) $k = 4$. In (a) the curves for S_{l}^2, S_{r}^2 and S_{int} are omitted and the total intensity is shown for $N = 47, 48, 50, 51, 52$ and 53 (from top to bottom at the central peak). The thick line is the average and it hides the $N = 50$ line. The lines for $N < 50$ have been dashed to make them visible near the main peaks.

is seen, the height of the central peak is very sensitive to the exact value of N, while the split peaks are hardly affected visually. The middle (thick) line is in fact the average over all lines from $N = 47$ to 53. It covers the $N = 50$ line almost completely, i.e. a narrow distribution of domain sizes does not smear out the interference effects significantly. This particular value

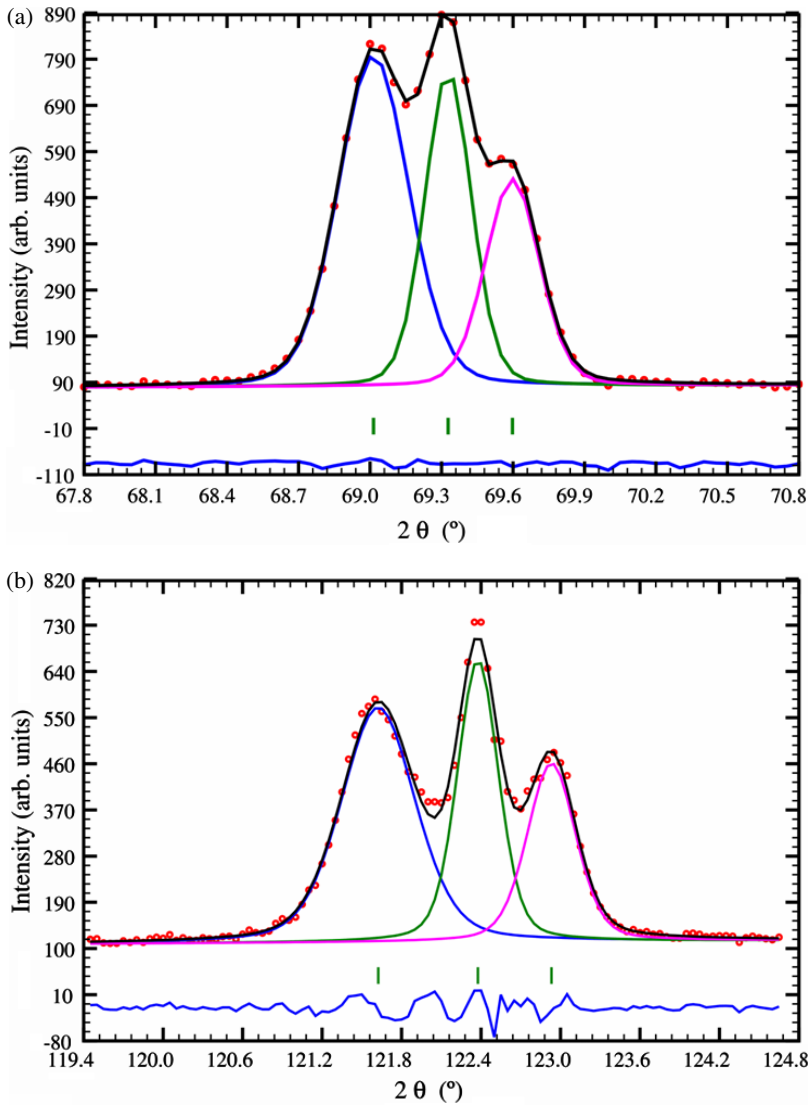

Figure 7. Experimental powder patterns (neutron diffraction, $\lambda = 1.5943$ Å) showing the $022_l/220_r$ (a) and $133_l/331_r$ (b) reflection groups (tetragonal indices).

of N has been chosen because the corresponding peak structure is reminiscent of that observed in an actual neutron powder diffraction measurement on $PbTiO_3$ at 740 K. Figure 7(a) shows the $022_l/220_r$ pair (tetragonal indices) which corresponds to $h_0 = 1$ and $k = 2$ (see (2) and figure 1(b)). The central peak has previously been assigned to the cubic phase coexisting with the tetragonal one at this temperature, but the comparison with figure 6 suggests that it could as well be an interference peak, as argued above. Note, however, that figure 6 refers to the reciprocal lattice, while figure 7 shows the powder average along 2Θ. A similar three-peak structure was observed for the $133_l/331_r$ pair (figure 7(b)). In this case adjacent twin reflection pairs are for example $13\bar{3}_l/331_r$ and $\bar{3}31_l/133_r$, which correspond to $h_0 = 2$, $k = -2$ and $h_0 = -1$, $k = 4$, respectively. Hence, two different forms of the interference pattern (those for

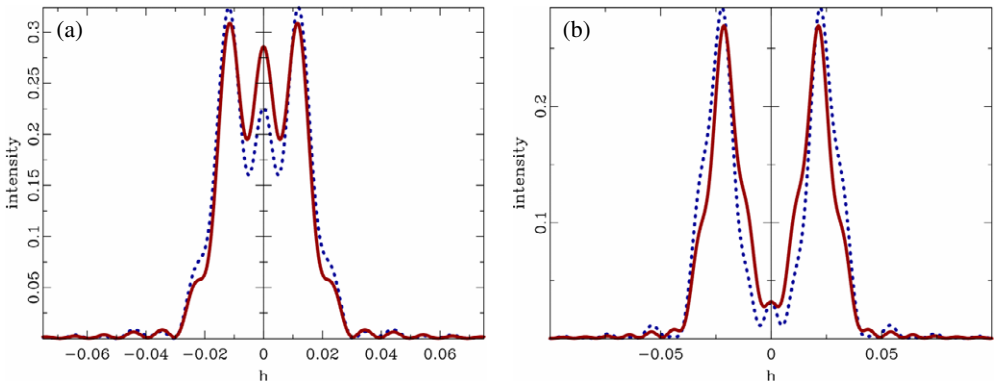

Figure 8. Comparison of total intensities with (solid lines, red) and without (dashed lines, blue) extended domain wall with $N_w = 10$ for $e = 0.012$, $N = 50$ and for (a) $k = 2$ and (b) $k = 4$.

$k = -2$ and 4, respectively; cf figures 6(a) and (b)) are superimposed for these symmetrically equivalent reflections, thus further complicating the analysis of the powder patterns.

The different widths of the peaks noticeable in figure 7 have been assigned to the strain variation within the domain wall by Boysen (2005). From this analysis a ratio $L/W = N/N_w$ of about 5 may be estimated at 740 K. According to this, figure 8 shows the alterations due to a finite domain wall width with $N_w = 10$. As expected, some intensity is shifted towards the centre, but the dominant influence of the interference term persists.

4. Conclusions

It has been shown that coherence effects may lead to significant modifications of the diffraction pattern, if domain structures occur on a mesoscopic scale. For small strains critical domain sizes may be as large as several hundreds of angstroms, which are not uncommon in real systems (Salje 1990). As mentioned, for a reliable interpretation of experimental data the structure factor variation along h and the smearing due to instrumental resolution have to be taken into account; both of which, however, will not conceal the coherence effects as long as they are as dominant, as in some of the examples above. Published assignments to multiple phases and higher or lower symmetries, as well as derived lattice constants and domain sizes, may have to be reconsidered under these aspects. In principle, they may easily be distinguished by following the scattering vector dependence of the reflections, since the coherence effects depend only on k, while the other cases have different index dependence. In practice, however, this may be not that easy because of limited instrumental resolution. In fact, in the example of the powder measurements of $PbTiO_3$ presented above it seems that there is indeed a coexistence of a cubic and a tetragonal phase, although from an estimation of the actual domain sizes and wall widths interference effects should be remarkable, unless they are destroyed by other effects like those mentioned in the introduction. On the other hand, if coherence effects can be detected unambiguously, they would allow a determination of both N and N_w and not only of the ratio N/N_w as in the statistical approaches of Taylor and Swainson (1998) and Boysen (2005).

The coherence effects are particularly serious when trying to interpret powder patterns, where small grain sizes tend to produce small extensions of the domains. Although these are usually much larger in single crystals, the decreasing and vanishing strains approaching ferroelastic phase transitions should induce such effects in this case too, at least close to T_c. Furthermore, mesoscopic domain structures arising from other processes, such as exsolution,

can lead to similar effects. As an example, the characteristic distribution of sharp and diffuse intensities observed in single-crystal x-ray diffraction experiments on enstatite has previously been interpreted qualitatively by out-of-phase lamellar domains of orthoenstatite (with a domain size of about 60 Å) intergrown with single layers of clinoenstatite (Boysen *et al* 1991). While trying to interpret recent more extended new data with this model quantitatively, problems have been encountered which are probably due to neglecting the coherence terms. Work is in progress to solve these problems. In summary, much more effort is required, in particular in the powder case, to carefully analyse one's data and finally arrive at unambiguous and sound conclusions. Moreover, further work is needed to investigate the possible reasons which seem to destroy the coherence effects in many real systems.

References

Andrews S R and Cowley R A 1986 X-ray scattering from critical fluctuations and domain walls in KDP and DKDP *J. Phys. C: Solid State Phys.* **19** 615–35

Barsch G R and Krumhansl J A 1984 Twin boundaries in ferroelastic media without interface dislocations *Phys. Rev. Lett.* **53** 1069–72

Boysen H 1995 Diffuse scattering by domains and domain walls *Phase Transit.* **55** 1–16

Boysen H 2005 Ferroelastic phase transitions and domain structures in powders *Z. Kristallogr.* **220** 726–34

Boysen H, Frey F, Schrader H and Eckold G 1991 On the proto- to ortho-/clino enstatite phase transformation: single crystal x-ray and inelastic neutron investigation *Phys. Chem. Minerals* **17** 629–35

Bruce D A 1981 Scattering properties of ferroelectric domain walls *J. Phys. C: Solid State Phys.* **14** 5195–214

Cowley J M 1976 Diffraction by crystals with planar faults. I. General theory *Acta Crystallogr.* A **32** 83–7

Cowley J M and Au A Y 1978 Diffraction by crystals with planar faults. III. Structure analyses using microtwins *Acta Crystallogr.* A **34** 738–43

Hayward S A and Salje E K H 2005 Diffuse Scattering from microstructures and mesostructures *Z. Kristallogr.* **220** 994–1001

Jacobs A E 1985 Solitons of the square-rectangular martensitic transformation *Phys. Rev.* B **31** 5984–9

Jagodzinski H and Frey F 1996 Disorder diffuse scattering of x-rays and neutrons *International Tables of Crystallography* vol B, ed U Shmueli (Dordrecht: Kluwer–Academic) pp 392–433

Khoshnevisan B, Ross D K, Broom D P and Babaeipour M 2002 Observations of twinning in $Yba_2Cu_3O_{6+x}$, $0 < x < 1$, at high temperatures *J. Phys.: Condens. Matter* **14** 9763–78

Salje E K H 1990 *Phase Transitions in Ferroelastic and Co-elastic Crystals* (Cambridge: Cambridge University Press)

Taylor D R and Swainson I P 1998 The diffraction spectrum of twinned domains: determination of domain wall width *J. Phys.: Condens. Matter* **10** 10207–13